Transport mechanisms as indicators of the durability of precast recycled concrete

F. Fiol [1], C. Thomas [2,*], J. M. Manso [1], I. López [3]

[1] Department of Construction, University of Burgos. EPS, Calle Villadiego s/n, Burgos, Spain; ffiol@ubu.es
[2] LADICIM (Laboratory of Materials Science and Engineering) University of Cantabria, E.T.S. de Ingenieros de Caminos, Canales y Puertos, Av/Los Castros, Santander, Spain; thomasc@unican.es
[3] Campus de Gijón, Department of Construction and Manufacturing Engineering, University of Oviedo, 33203 Asturias, Spain; inigo2208@hotmail.com
* Correspondence: thomasc@unican.es

Abstract:

The objective of this paper was to analyze the influence of crushed precast concrete waste on the transport mechanisms as indicators of the durability of precast recycled self-compacting concrete (SCC) as an alternative to the coarse fraction of natural aggregate. The replacement percentages were 20%, 50% and 100%, by weight, of the silica gravel 2/12.5 mm. Two types of SCC were manufactured: the first with a minimum compressive strength of 30 MPa (HR-30) and the second with a minimum strength of 45 MPa (HR-45). The recycled SCC's mechanical characteristics such as compressive strength, splitting tensile strength, flexural strength and modulus of elasticity were analyzed. Regarding the physical properties related to transport mechanisms, the influence of the recycled aggregate on the porosity, absorption, penetration of water under pressure, density of hardened concrete and ultrasonic pulse velocity was analyzed. All these properties were compared with those of a control concrete. The results of the mechanical tests provide values close to those obtained for the control SCC, while, in terms of durability the results fulfil the limit values that are considered for a good quality concrete. Therefore, it can be concluded that the use of crushed precast concrete waste with different degrees of substitution is a viable alternative in the manufacture of more sustainable SCC.

Keywords: Recycling; Mechanical testing; In-fresh properties; Recycled aggregate concrete; Precast; Self-compacting concrete.

1. Introduction

The construction industry and all those related to cement derivatives consume a large amount of natural resources. The extraction of natural aggregates used for the manufacture of mortars and concrete is subject to growing problems due to the depletion of the quarries, the negative impact it produces on the environment and regulatory requirements. Within this sector the use of prefabricated elements has become consolidated over the years. Although these types of products have more impact internationally, in countries such as EEUU, Canada or Japan, in some European Union (EU) countries, such as the Netherlands and Germany, the prefabrication industry accounts for above 35% [1]. For these reasons, at the international level, different strategies are being established which go beyond the current legislation that aims to make precast firms carry out actions that increase sustainability in the precast industry. Regarding these strategies, it is worth noting the "Precast Sustainability Strategy and Charter" of the British Precast Concrete Federation [2], membership of which has been obligatory in Britain since 2014. In addition, prefabrication companies from EU and in compliance with EU Regulation 305/2011 of Construction Products [3] will have to comply with the "Sustainable use of natural resources" requirement, so construction work must be designed, built and demolished in such a way that the use of natural resources is sustainable.

Taking into account that aggregates make up approximately 80% of the total volume of concrete and their extraction is causing the depletion of these natural resources and generating different

environmental problems, the reuse of Construction and Demolition Wastes (CDW), as substitutes for natural aggregate in the manufacture of concrete, could provide a viable alternative to reduce the overexploitation of natural aggregate quarries and their impact on the environment.

In recent decades, numerous studies have been carried out with the objective of analyzing the influence of the incorporation recycled aggregates (RA) on the properties of concrete [4–8]. In general, these works show a decrease in the physical and mechanical properties and durability of concrete. C. Thomas et al. [5,7,9–14] analyzed the physical and mechanical properties, including fatigue behavior, and durability of concrete incorporating recycled aggregate (RA) in aggressive environments. Moreover, they employed steel slag aggregate as a special RA [15]. They observed a greater influence of RA for concretes with high w/c ratios and a decrease in durability due to the intrinsic porosity of RA, although these differences compared with the control concrete decrease for low w/c ratios. The results obtained by Miguel Bravo [6] also showed a reduction in concrete properties by incorporating processed waste from different CDW recycling plants. Although the results were more dispersed depending on the type of RA and its composition.

As for compressive strength, there are numerous studies demonstrating that it decreases as the percentage of RA present in the mixture increases. Several authors set percentages of resistance reduction whose range of values is between 0-5% for a replacement of 20%, 5-15% for a replacement of 50% and up to 30% for the incorporation of 100% RA [16–18]. It is estimated that this reduction is due to the lower resistance of the aggregates and the increasing presence of weak areas in the concrete. However, the incorporation of 20% of RA is acceptable, even percentages greater than 50% are acceptable if the water/cement ratio is kept constant and the lower workability is compensated through the use of superplasticizers.

The durability of concrete is another factor that can be affected by the incorporation of RA, being reduced as the percentage of recycled aggregate present in the mixture increases [5,19]. Although, when the concrete is exposed to aggressive environments it has been proven that the variations in durability, with respect to control concrete, are smaller [7]. However, there are discrepancies because some authors such as Olorunsogo [20] and Kou [21], conclude that durability can significantly improve with the age of cure. In relation to the conclusions obtained in these studies, it is possible to affirm that the durability characteristics may be more influenced by the water/cement ratio, so the influence of recycled aggregates on properties such as concrete permeability, which is closely connected with durability, would not be considered significant [16]. C. Thomas et al. [12] showed that the durability of concrete is also influenced by the degree of saturation of the RA. The results show a greater porosity when the aggregates that are incorporated into the mixture are saturated. M. Martín-Morales [22] analysed the feasibility of using recycled concrete aggregates for the production of hollow concrete blocks. The results show adequate durability of hollow concrete blocks against certain extreme environmental conditions such as freeze-thaw and salt crystallization.

Another alternative may be the incorporation of RA in the manufacture of self-compacting concrete (SCC). Thanks to its great capacity for self-consolidation, concrete without voids, more waterproof than traditional ones and with excellent surface finish is obtained. The use of this type of concrete is widespread in the prefabrication industry. Therefore, in recent years numerous studies have been carried out where the feasibility of incorporating different types of RA into the SCC is analyzed [11,23–25]. Jose Sainz-Aja et al. [11] analysed the possibility of recycling out-of-service railway superstructure wastes as RA in the manufacture of SCC and with them achieve different environmental benefits. Kou and Poon [23] evaluated the fresh and hardened properties of SCC using recycled concrete aggregate as both coarse and fine aggregates. The results do not show very relevant differences between the control SCC and the SCC with fine recycled concrete aggregate.

As can be seen, although these studies focus on the use of different wastes in the manufacture of SCC, there are few studies related to the use of waste from the prefabricated industry and its incorporation back into the manufacturing process. T. Barroqueiro et al. [26] confirmed the viability of producing e high-performance self-compacting concrete with recycled aggregates from the precast industry. In this regard, also, F. Fiol [13] assessed the influence of incorporating recycled aggregates

from prefabricated elements on the mechanical properties of SCC, obtaining results close to those of control concrete.

The use of this waste and its incorporation back into the production chain, in addition to achieving economic savings, contributes to the sustainability of the sector. If the latest technologies are also applied, the result can be doubly beneficial. For all these reasons, the main objective of this study was to analyze the feasibility of using recycled aggregates from precast elements to produce a self-compacting structural concrete, with compressive strengths of 30 and 45 MPa and with percentage substitution of 20%, 50% and 100% by weight of natural aggregate. To evaluate the influence of the RA on the behavior of the manufactured SCC, different physical and mechanical tests were performed. This is an innovative study as up to date, because although there are studies that analyze the influence of use of concrete waste in the manufacture of concrete, few are the studies that focus on the use of waste from the precast sector [13,27–29] and fewer that use this type of waste in SCC [13,26,29]. These studies analyse the influence of waste from the precast concrete industry on the physical and mechanical properties of SCC, while our study aims to analyse the influence of this type of waste on the transport mechanisms that affect durability of recycled concrete.

2. Materials and Methods

2.1. Materials

The cement used in this research was CEM I- 52.5 R. Table 1 shows its main characteristics. Two types of natural aggregates were used: 0/2 mm silica sand as the finest aggregate while, as a coarse aggregate, a silica gravel with a size of 2/12.5 mm was used. The apparent density and water absorption of the aggregates was determined following the specifications of the UNE-EN 1097-6 standard [30]. The 0/2 mm sand has a density of 2640 kg/m^3 and an absorption coefficient, by weight, of 0.26%, while, the gravel 2/12.5 mm has a density of 2680 kg/m^3 and a coefficient absorption of 1.16%. Their grading curves are shown in Fig. 1. Addition limestone filler, produced in BELCHITE (Zaragoza, Spain) and complying with the ISO 9001 certificate, was used.

In order to achieve suitable workability of self-compacting concrete (SCC), two polyplacarboxylate superplasticizer additives were used. The superplasticizers used were: Sika ViscoCrete®-20 HE, especially suitable for the preparation of concrete with high initial strength, concretes with great need for water reduction and excellent fluidity, and Sika ViscoCrete®-5920 HE, a high-performance superplasticizer that is usually used in concrete with low water content. Finally, as recycled aggregate (RA) and alternative to coarse aggregate, crushed precast concrete waste with a size of 4/12.5 mm was used.

Table 1. Cement chemical composition.

Test	Average result (% by weight)
Loss on ignition (LOI)	1.0
Insoluble residue	0.6
Sulphates SO_3	3.1
Chlorides	0.03
Alkali content	0.7-0.8

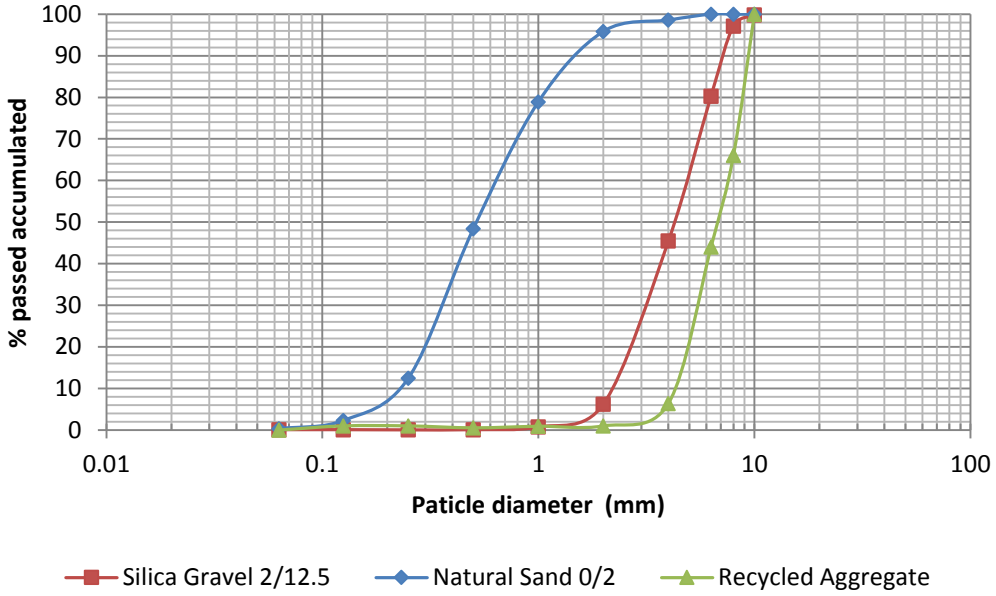

Fig. 1 Grading curves of silica gravel, natural sands and RA.

2.2. Recycled aggregates

The RA used in this study was obtained from useless precast elements; for works not executed, nonconforming pieces, pieces with erroneous geometry or from leftover wastes of the daily concreting. Some examples of the precast components Fig. 2.

To obtain the final RA used in this study, the following steps were followed: first, the pieces were crushed by a hydraulic clamp in order to eliminate the reinforcement, obtaining an aggregate size of 0/300 mm. Then, a first crushing process was performed by jaw crusher until a maximum aggregate size of 80 mm is obtained. Finally, the RA is processed in an impact crusher to reduce the size of the aggregate to 0/25 mm. The fraction used in this study to make concrete was 4/12.5 mm. Table 2 shows the main properties of the recycled aggregate used in this study. All results fulfil the requirements of EHE-08 [31]. The chemical composition of RA was determined by X-ray fluorescence analysis. Table 3 shows the corresponding results, while in Fig. 1 the grading curve of the RA is shown, together with the curves of the natural aggregates

Fig. 2. Rejected precast products.

Table 2. Physical and chemical properties of the RA.

Property	**Value**	EHE-08 [31]	Standard
Fines content (%wt.)	0.41	< 1	UNE-EN 933-1 [32]

Property	**Value**	EHE-08 [31]	Standard
Sieve modulus	6.68	-	UNE-EN 933-1 [32]
Flakiness index (%wt.)	7.90	<35	UNE-EN 933-3 [33]
Shape coefficient (%wt.)	2.25	UNE -933-4 (>0.2)	UNE-EN 933-4 [34]
Density (kg/m^3)	2410	-	UNE-EN 1097-6 [30]
Los Angeles (% wt.)	37	<40	UNE-EN 1097-5 [35]
Absorption coefficient (% wt.)	4.15	< 5	UNE-EN 1097-6 [30]
Chloride content (% wt.)	0.0005	< 0.05 HA >0.03 HP	UNE-EN 17744 [36]
Frost loss (% wt.)	11.51	<18	UNE-EN 1367-2 [37]
Sulphate content (%wt.)	0.50	<0.8	UNE-EN 17744 [36]
Soluble sulphates (%wt.)	7.07	-	UNE-EN 17744 [36]
Crushing value (%wt.)	35.42%	-	UNE-83112 [38]
Lost by calcination (% wt.)	0.47	-	UNE-EN 17744 [36]

Table 3. Chemical composition (%) of RA.

CaO	SiO_2	Al_2O_3	Fe_2O_3	SO_3	K_2O	MgO	TiO_2	C
37.4	56.53	2.16	1.1	0.16	1.32	0.79	0.098	0.47

2.3. Self-compacting concrete design

To carry out this study, two reference mixes were designed, HR-30 and HR-45, which ensure self-compacting fresh concrete. These control mixtures set a starting point for the mix proportions of precast recycled concrete and meet the standards that are commonly used in precast concrete plants. Once the control mix proportions were established, 20%, 50% and 100% of the natural coarse aggregate was replaced by the same volume of RA. Table 4 shows the mix proportions of each of the manufactured SCCs, in kg/m^3.

The incorporation of RA, as substitute of the natural one, shows influence on the effective water/cement ratio during the mixing process due to the high absorption coefficient of them. In order to adequately compare the properties analyzed in the experimental program, the effective water/cement ratios of each of the dosages used were calculated, estimating that the RA reaches approximately 70% water saturation capacity [39]. The calculation of the effective water/cement ratios is obtained from equation (1), while the effective water/cement ratios $(w/c)_{eff}$ can be seen in Table 4.

$$\left\{\frac{w}{c}\right\}_{eff} = \frac{W - \frac{0.7}{100}\sum_i (P_i A_i)}{c}, \quad (1)$$

where, $\left\{\frac{w}{c}\right\}_{eff}$ is effective water/cement ratio ; W is the total amount of water incorporated in the mixer; P_i is the weight of the components incorporated during mixing; A_i is the absorption of the components incorporated during.

The experimental program includes a total of eight mixes. Two of them correspond to the control SCC, HR-30-0% and HR-45-0%. The rest of the mixes correspond to SCCs with different contents of RA (Table 4).

Table 4. SCC mix proportions (kg/m^3).

Material	HR-30-0% Control	HR-30-20%	HR-30-50%	HR-30-100%	HR-45 0% Control	HR-45-20%	HR-45-50%	HR-45-100%
RA 4/12.5	0	250	540	1040	0	250	540	1040
Sand 2/12.5	1150	920	540	0	1150	920	540	0
Sand 0/2	650	650	670	720	650	650	670	720
Limestone filler	320	320	320	320	280	280	280	280
CEM I-52.5 R	250	250	250	250	320	320	320	320
Water	112	112	112	112	112	112	112	112
Sika 20HE	0.50	0.50	0.65	0.85	0.50	0.50	0.65	0.85
Sika 5920	1.30	1.30	1.60	2.00	1.50	1.50	1.80	2.20
w/c $_{eff}$	0.40	0.39	0.35	0.32	0.31	0.30	0.28	0.25

2.4. Experimental program

For mixing, the procedure stipulated in ASTM C192 [40] was followed, which was as follows: first, the mixer is wetted and coarse aggregates are added. Then half of the mixing water is incorporated. After that, the limestone filler and cement are added and the mixing process is started by adding the rest of the water, mixing for 3 minutes, the mixer is stopped and the mixture stands for 3 minutes. Finally, the mixer is activated and the mixing is continued for 2 more minutes. After this time the mixing process is finished.

Standardized specimens of the following dimensions were manufactured for each batch: 15×30 cm cylindrical specimens, 10×10×10 cm cubic specimens and 10×10×40 cm prismatic specimens. The specimen molds were filled according to the specifications of the UNE-EN 12350-1 standard [41]. The specimens were cured for 28 days in a humid chamber at a temperature of 20 ± 2 ° C and a relative humidity of 95% according with the specifications of the UNE-EN 12390-2 standard [42].

2.4.1. Mechanical properties

The following mechanical properties were determined: the consistency of fresh SCC according to UNE-EN 12350-8 [43] standard, compressive strength (UNE-EN 12390-3) [44], splitting tensile strength (UNE-EN 12390-6) [45], flexural strength (UNE-EN 12390-5) [46] and modulus of elasticity (UNE 83316) [47]. To determine flowability, fresh concrete is poured into a cone similar to that used in the slump-flow test of the EN-12350-2 standard [48]. When the cone is removed upwards, the time from the start of the extraction until the concrete flow reaches a diameter of 500 mm is measured, this being the time t_{500}. Next, the largest diameter of the extended SCC and the diameter perpendicular to it are measured and the average is the slump-flow.

2.4.2. Durability properties

Regarding durability, the following properties were determined: porosity and absorption of hardened concrete according to the specifications of ASTM C-642 [49], penetration of water under

pressure according to the specifications of UNE-EN 12390-8 [50], density of hardened concrete according to UNE-EN 12390-7 [51] and ultrasonic pulse velocity by UNE-EN 12504-4 [52].

2.4.3. Micro and macro-porosity analysis

To quantitatively assess the macroporosity of the concretes used, pores larger than 170 μm, computed axial tomography (TAC) was used. The equipment consists of an X-ray system with a 225 kV / 30mA Yxlon tube, with a metallic steel-lead-steel cabin, so that it operates with a maximum radiation of 225 kV / 30mA (within the booth), the maximum radiation dose at a distance of 100 mm from its external surface does not exceed 2.5μS / h. The software that regulates the instruments coordinates the number, thickness and number of sections on the specimen under consideration (Fig. 3 Test tube and programming of the number and thickness of the cross sections.).

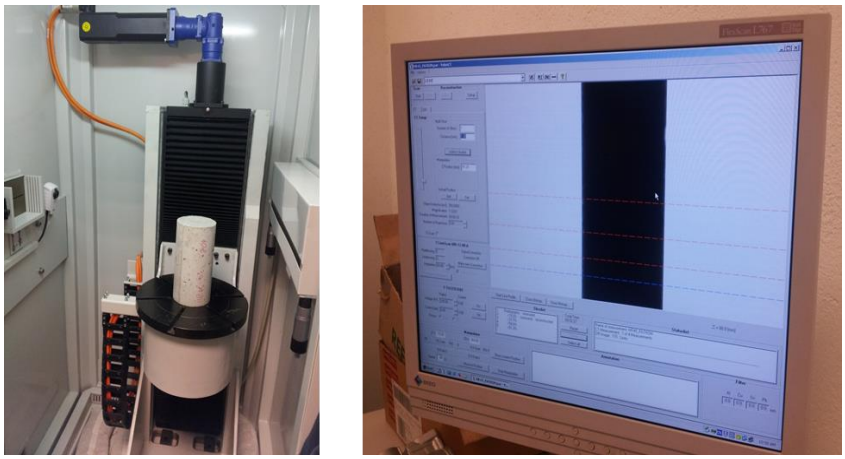

Fig. 3 Test tube and programming of the number and thickness of the cross sections.

The methodology for evaluating macroposity was carried out using the VgsStudio Max (Vgs Studio Max version 2.2 High-end software for the visualization and analysis of industrial CT data) and Mimics software (Mimics V 10.0. Materialises Interactive Medical Image Control System. Version 10.0). In the first one, several sections corresponding to circular sectors are made on a cylindrical specimen to differentiate and relate the volume of pores from the outside to the inside.

The determination of porosity by mercury intrusion porosimetry (PIM), analyzes the micropores of the material. The operating procedure begins by vacuuming the samples, and then applying a hydrostatic pressure with mercury to the chamber containing the sample. The mercury intrusion pressure is inversely proportional to the pore opening size. The applied pressure values and the volume of mercury intrusion give graphical representations of the filling process, which enables the representation of the cumulative volumes, differentials and percentage porosity estimated from the Washburn equation that assumes cylindrical pore volumes. The Washburn equation describes the balance between the internal and external forces of a three-phase solid-liquid-vapor system.

Three fundamental parameters are obtained in the PIM: the total porosity, the pore diameter and the distribution of the porous structure. Total porosity is the volume of pores with respect to the total volume, where only the connected pores are considered, according to expression.

$$P_t = \frac{V_p}{V_m} x100 \quad (2)$$

Where

P_t Total porosity (%).

V_p pore volume (mm^3).

V_m volume of material (mm^3).

The average pore diameter is the corresponding diameter assuming an equivalent cylindrical distribution, and is determined according to the equation:

$$\emptyset = \frac{4\,V}{A} \tag{3}$$

$\emptyset$ average pore diameter.
V pore volume (mm^3).
A material's surface.

3. Results and analysis

Table 5 shows a summary of the results obtained in this study. All values, except slump and ultrasonic pulse velocity (UPV), correspond to the average value of the three results obtained in each of the tests performed. The characterization of the hardened concrete was carried out after curing the specimens for 28 days.

3.1. Flowability

Table 5 shows the results obtained for the different SCCs. A reduction in workability can be observed when the RA replaces natural aggregate 2/12.5 mm. This decrease occurs for all replacement percentages, including for ratios of 50% and 100% where the amount of additive was increased. This may be due to the greater absorption of water by the RA, of 4.15%, with respect to the aggregate 2/12.5 mm, of 1.16%. This entails a reduction in the effective water/cement ratios (w/c) and, therefore, in the workability of the SCC.

Table 5. Results of the experimental program.

Test	HR-30-0%	HR-30-20%	HR-30-50%	HR-30-100%	HR-45-0%	HR-45-20%	HR-45-50%	HR-45-100%
Flowability (cm)	68	60	58	55	75	71	60	65
Compressive strength (MPa)	49.09	49.98	55.34	56.75	63.36	64.13	66.82	72.81
Splitting tensile strength (MPa)	5.17	5.06	4.85	4.92	5.30	5.21	4.95	5.00
Flexural strength (MPa)	6.20	6.30	6.30	5.60	7.95	7.80	7.80	7.50
Modulus of elasticity (GPa)	36.98	38.50	35.15	34.03	40.83	42.60	38.01	37.80
Open porosity (%vol.)	7.30	7.50	8.15	8.50	5.15	5.80	6.00	6.30
Absorption (%wt.)	3.30	3.40	3.80	4.10	2.95	3.00	3.20	3.01
Water penetration (mm)	10.0	12.8	13.5	11.5	12.0	8.6	15.0	14.5

3.2. Compressive strength

Table 5 shows the average compressive strength values obtained for HR-30 and HR-45 concretes with substitution of 0%, 20%, 50% and 100%. The results show an increase in compressive strength

as the percentage of RA increases. However, this may be due to the increased absorption of RA, which reduces the effective w/c ratio [5]. However, it is also well-known that the behavior of compressive strength as a function of the w/c ratio can be fitted to an exponential curve with equation (4) [5,53,54]:

$$y = Ae^{-B(\frac{w}{c})}, \quad (4)$$

where, y is compressive strength for a cured age; w/c is the effective water/cement ratio; A and B are the parameters to be calculated.

Considering the results obtained, the corresponding parameters were calculated. Fig. 4. Compressive strength of SCC as a function of the w/c ratio. shows the compressive strength curves of the different SCC, at 28 days, against the effective water/ cement ratio.

Once these parameters were calculated, and as can be seen in Figure 3, as the w/c ratio decreases there is an increase in compressive strength. These results are in line with those obtained in other studies [5,23,39,55,56]. Regarding the substitution ratio, the results show a slight loss of compressive strength for the same w/c ratio as the substitution percentage is increased. However, for a ratio of 20% the variation with respect to the control SCC is not significant.

Finally, the confluence of the curves was noted as the w/c ratio is increased. This may be because the lower resistance of the recycled aggregate compensates for?? the worst paste quality for the high water/cement ratios. For low water/cement ratios the opposite happens, the difference between the control concrete and the concrete with RA is higher, which denotes the good quality of the new paste. The results of the compressive strength shown in Table 5, where the dosage in the recycled concrete is maintained, are in the line with the results obtained in other studies [57,58]. The higher water absorption of the RA results in a lower w/c ratio, which causes an increase in strength.

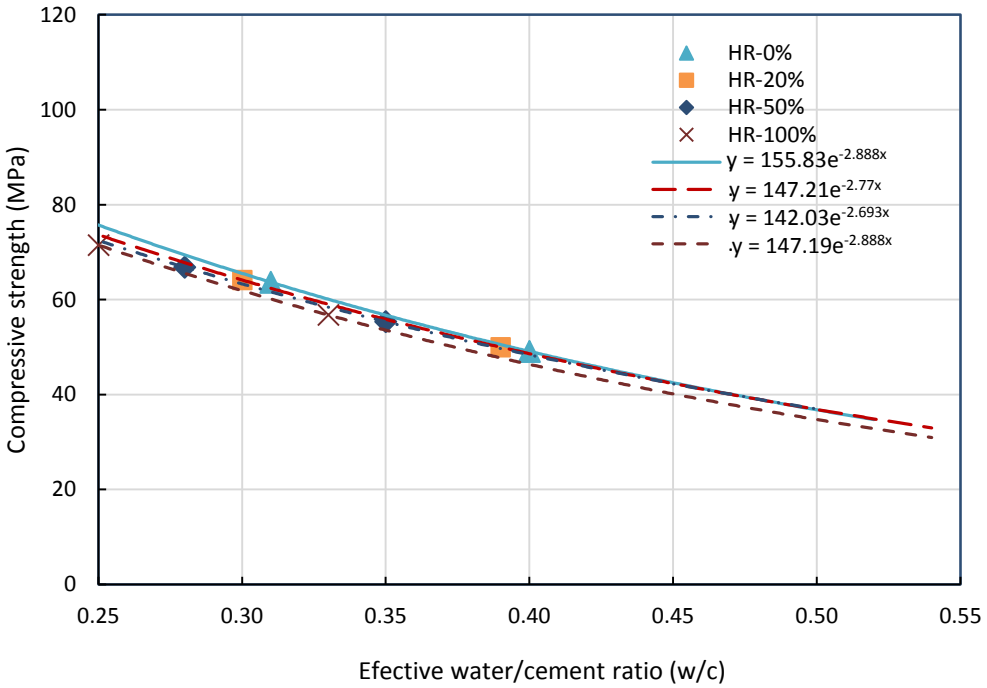

Fig. 4. Compressive strength of SCC as a function of the w/c ratio.

3.3. Splitting tensile strength

The tensile strength values are shown in Table 5 and are represented in Fig. 5. Splitting tensile strength of SCC as a function of the w/c ratio., respectively. As in the case of compressive strength values, the values can be adjusted according to equation (4). The results show a decrease in splitting tensile strength as the replacement percentage is increased, although the variations are small. The variation between the control SCC and the SCC with a ratio of 100% RA indicates a strength loss of 4.8% for the HR-30 and 3.7% for the HR-45.

These results are well below the results obtained in other studies where there is a large dispersion in the results observed. The studies carried out by Sanchez and Alaejos [59] show a high dispersion in the values, which range between -20% and + 20% depending on the type of waste used. These differences may be related to the quality of the RA used.

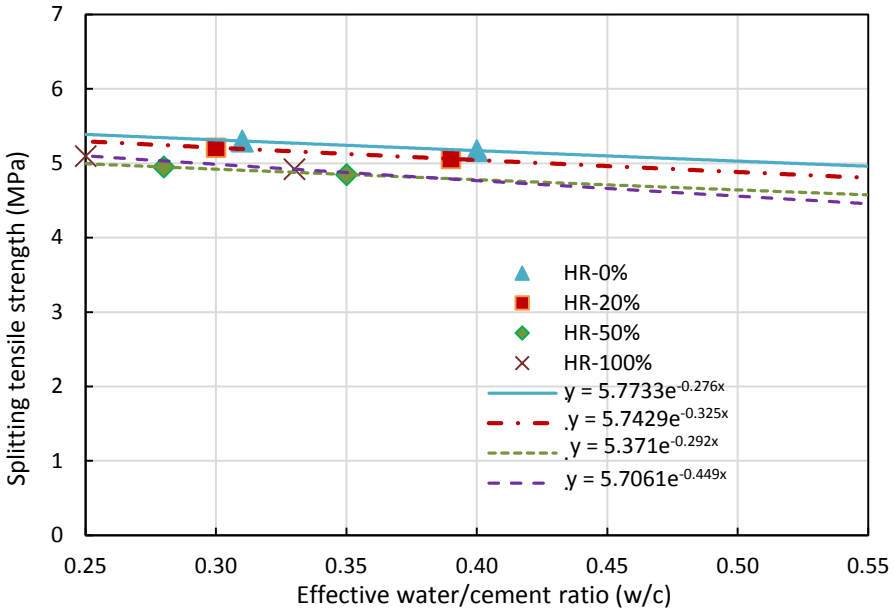

Fig. 5. Splitting tensile strength of SCC as a function of the w/c ratio.

3.4. Flexural strength

Table 5 shows the average results of flexural strength of the SCC with RA for the different types of HR-30 and HR-40, while, Fig. 6 shows the relationship between the flexural strength and the effective w/c ratio. As in the previous cases, the values were adjusted according to equation (4). In this case, compressive strength curves tend to converge when the effective w/c ratio increases.

The results for 20% substitution show little variation and it can even be seen that the trend line is reversed for values of w/c greater than 0.4. Fig. 6 also shows a decrease in strength as the w/c increases and also a decrease as the degree of substitution. For 100% ratios, the flexural strength losses vary between 3% and 4%. These values are considerably lower than those found by Sánchez and Alaejos in [29], where the percentages ranges between ± 20%. As mentioned above, our better results may be a consequence of the higher quality of our RA.

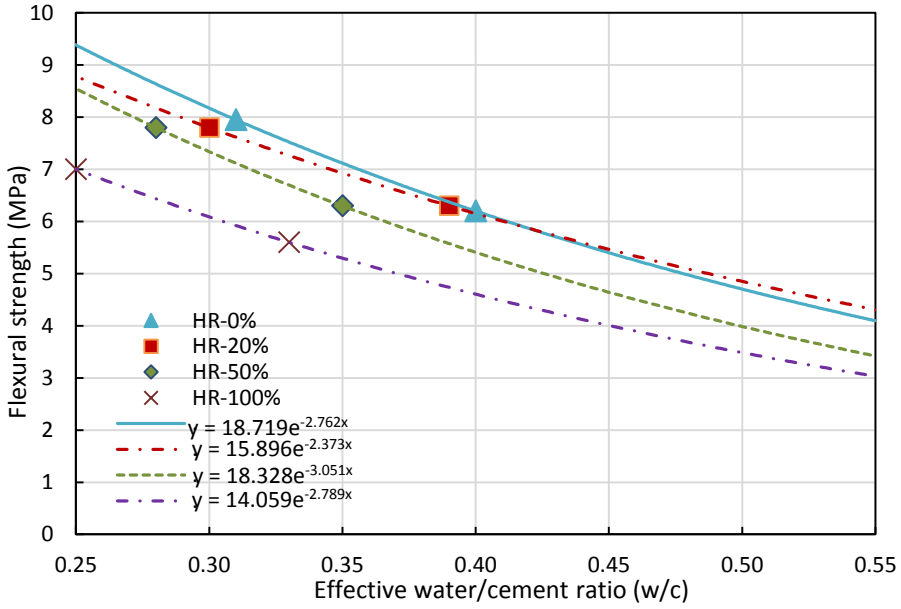

Fig. 6. Flexural strength of SCC as a function of the w/c ratio.

3.5. Modulus of elasticity

The average values of the static modulus of elasticity are shown in Table 5 Fig. 7. Static modulus of elasticity of SCC as a function of the w/c ratio. the variations in the modulus of elasticity as a function of the effective w/c ratio. In this case, the values can be fitted to a line, with equation (5) [5]:

$$y = Ax + B, \quad (5)$$

where, y is the modulus of elasticity; x is the effective water/cement ratio; A and B are parameters to be calculated.

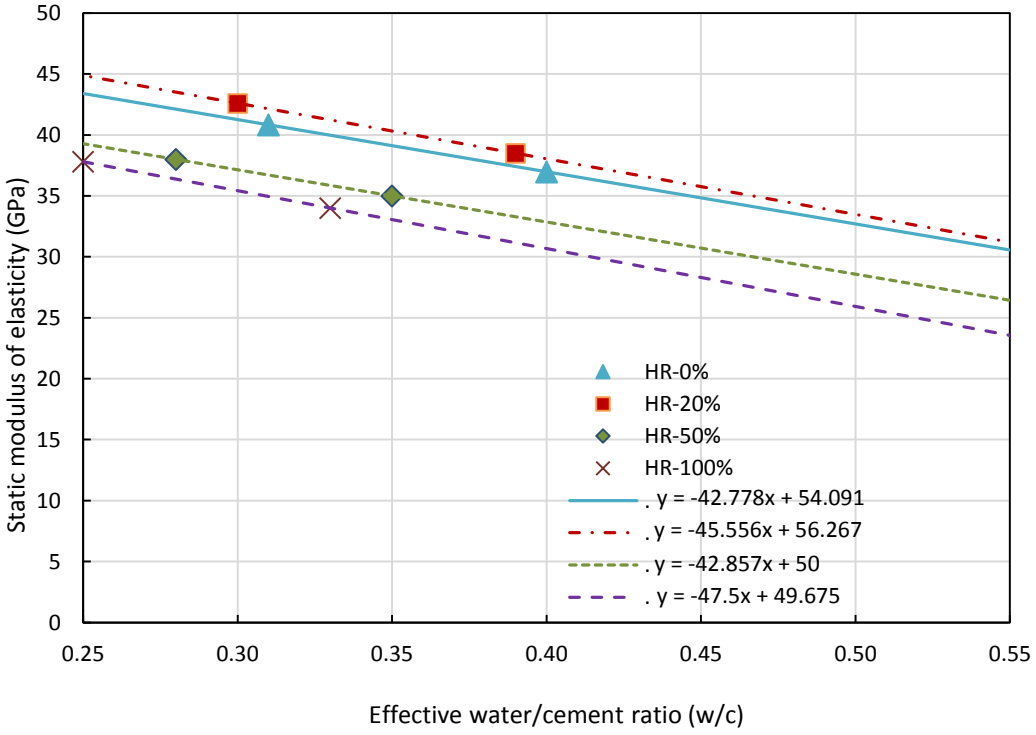

Fig. 7. Static modulus of elasticity of SCC as a function of the w/c ratio.

As expected, the modulus of elasticity decreases when the ratio of RA increase. This may be due to the greater porosity and the greater volume of cement adhered to the recycled aggregate with respect to the natural aggregate producing greater deformability of the concrete [27]. For 20% substitution, the values are very similar to the control SCC, becoming practically the same results for high w/c ratios. However, for a substitution of 50% and 100% a loss of strength is observed, of between 7-10% with respect to the control SCC. These results are in line with those obtained in other studies [27,39,60]. Soares et al. [27] observed a reduction of 11% in the modulus of elasticity when replacing 100% of coarse aggregate with recycled aggregates from precast concrete wastes.

3.6. Open porosity and absorption

In this study, the influence of the incorporation of RA on open porosity and the absorption of SCC for concrete type HR-30 and HR-45 was analyzed. Table 5 shows the values obtained and Fig. 8 and Fig. 9 show the variations in porosity and absorption of the SCC as a function of the effective w/c ratio. As has been shown in several studies [5,53], both porosity and absorption as a function of the w/c ratio respond to a logarithmic curve. This curve can be fitted to the following equation (6).

$$y = A\ Ln(x) + B, \quad (6)$$

where, y is open porosity or absorption; x is the effective water/cement ratio; A and B are parameters to be calculated.

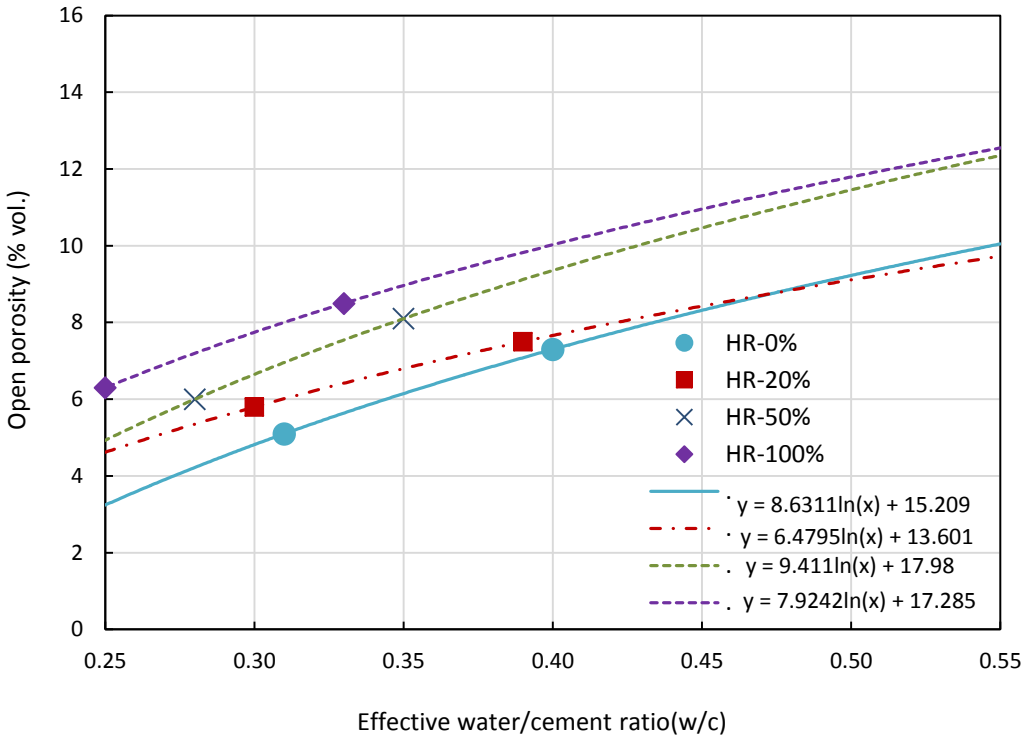

Fig. 8. Open porosity of SCC as a function of the w/c ratio.

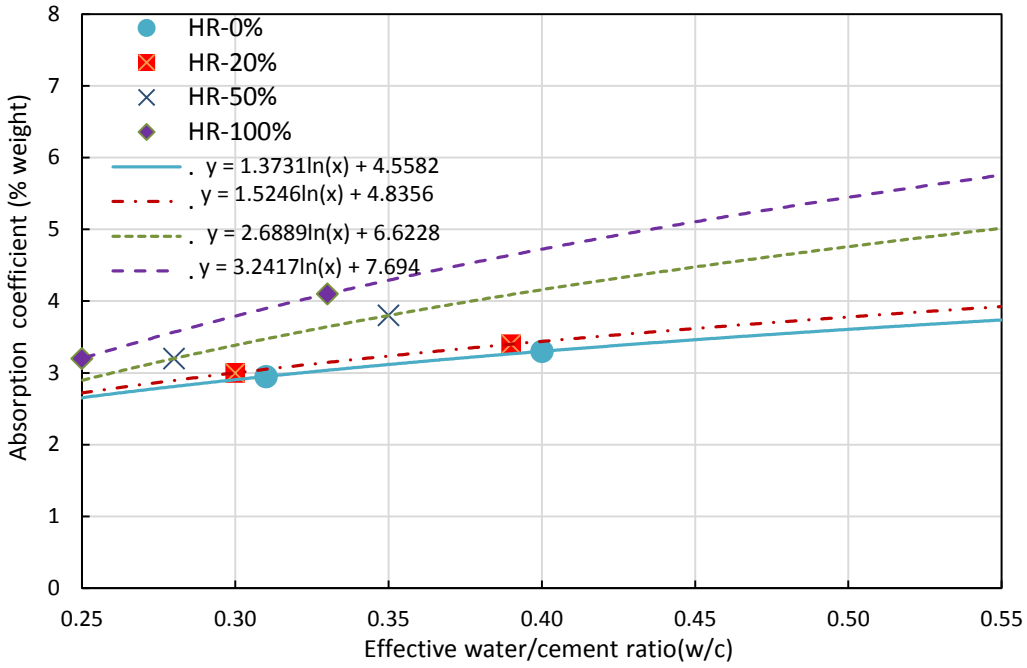

Fig. 9. Water absorption of SCC as a function of the w/c ratio.

The results in Table 5 show an increase in the absorption and open porosity of the SCC as the percentage of RA increases replacing natural aggregate 2/12.5 mm. As mentioned before, in similar studies [25], the increased water absorption of the SCC with RA is a logical consequence of the greater absorption of water by the recycled aggregate compared to natural aggregate. For open porosity, all values are below the 15%, limit value assumed for a concrete to be considered of good quality [61]. For high replacement percentages, 50% and 100%, an increase in porosity between 11 and 23% is observed. For ratios of 20% the variation is small. In Fig. 8 it can be seen that as the w/c ratio is increased, the porosity of the SCC increases.

The curves showing water absorption as a function of the effective w/c (Fig. 9) indicate that the greater the w/c ratio, the higher is the influence of the RA on the water absorption coefficient, . A greater slope in the SCC is observed with ratios of the 50% and 100% of RA. This may be because the less absorbent concrete pastes, the ones with the lowest w/c ratios, isolate the porosity and lessen the effect that the RA has on absorption.

The absorption and porosity results obtained are in line with the results of other studies [5,7,13]. In all of them it is observed that for the same w/c ratio there is an increase in both the porosity and the absorption as the percentage of RA increases.

Finally, Table 5 shows a greater absorption in concretes with lower strength (HR-30). This is due to the evolution of the pores produced by the recrystallization of the cement components that produce a favorable effect by filling a large part of them [5,62].

3.8. Water penetration

The average results of water penetration under pressure are shown in Table 5. The results show an increase in values for SCC with RA. However, all values are below the average depth limit (20 mm) set in the EHE for the most demanding exposure environments [31]. Therefore, it can be said that the SCC is sufficiently waterproof.

Fig. 10 shows the relationship between the values of water penetration under pressure as a function of the effective w/c ratio. These values can be fitted to a logarithmic curve like the one in equation (6). For a substitution of 20% there are hardly any variations with respect to the control SCC, regardless of the ratio of w/c. For 50% and 100% ratios, an increase in water penetration is observed,

which becomes more evident as the w/c ratio is increased. However, when the effective w/c ratio is low, 0.25 to 0.30, the curves tend to converge to water penetration values between 15 and 20 mm.

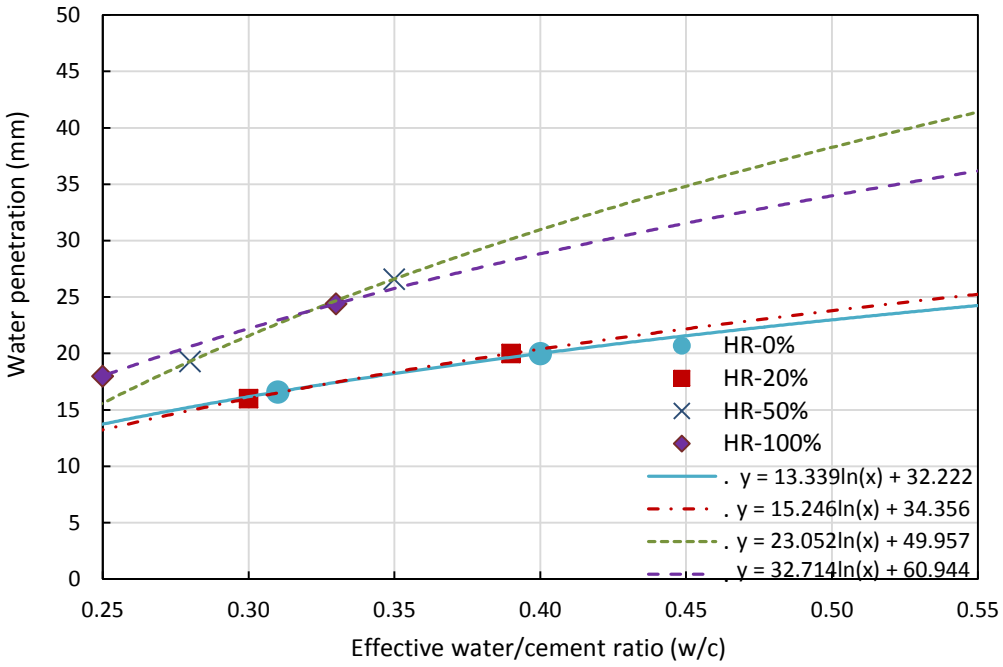

Fig. 10. Water penetration of SCC as a function of the w/c ratio.

3.9. Ultrasonic pulse velocity

The results of the ultrasonic pulse velocity (UPV), for the different percentages of RA as a function of the effective ratio w/c can be seen in Fig. 11. The values are fitted to a line like equation (5). In line with similar studies [56], the lower is the w/c ratio, the higher is the propagation speed of ultrasonic waves. In addition, the analysis of the graph shows that the incorporation of RA, with equal effective w/c ratio, implies a decrease in the speed of the ultrasonic impulses in the same way as the degree of substitution. For a ratio of 100% a decrease in the UPV of 5% can be seen. However, the values obtained can be considered excellent, as they are all above 4.50 km/s [63].

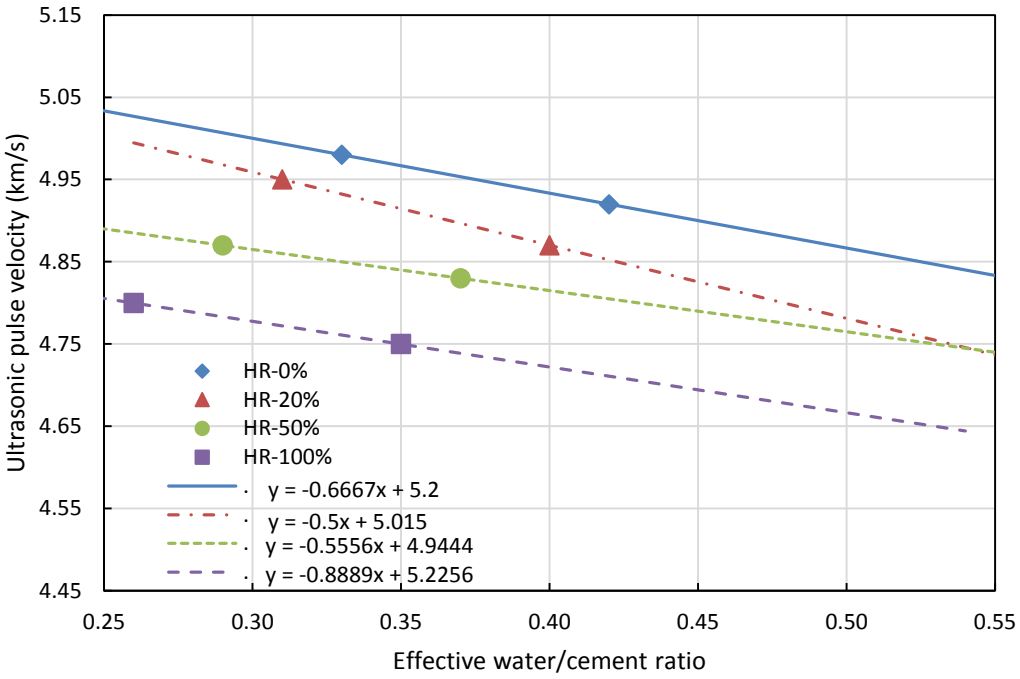

Fig. 11. Ultrasonic pulse velocity of SCC as a function of the w/c ratio.

3.10. Density of hardened SCC

Fig. 12 shows the density of hardened SCC for each percentage of substitution as a function of the effective w/c ratio. First, it is observed that the density increases linearly as the w/c ratio decreases according to equation (7) [13,39,59]:

$$y = Ax - B, \quad (7)$$

where, y is density; x is the effective water/cement ratio; A and B are parameters to be calculated.

It can be seen that as the percentage of RA increases there is a decrease in the density of SCC. These results are a consequence of the lower particle density of recycled aggregate, 2410 kg/m^3, compared to natural aggregate 2/12.5 mm, 2680 kg/m^3. These variations in the hardened concrete density are in line with the results obtained in other studies where precast concrete waste has been used as an alternative to natural aggregate [13,16,64].

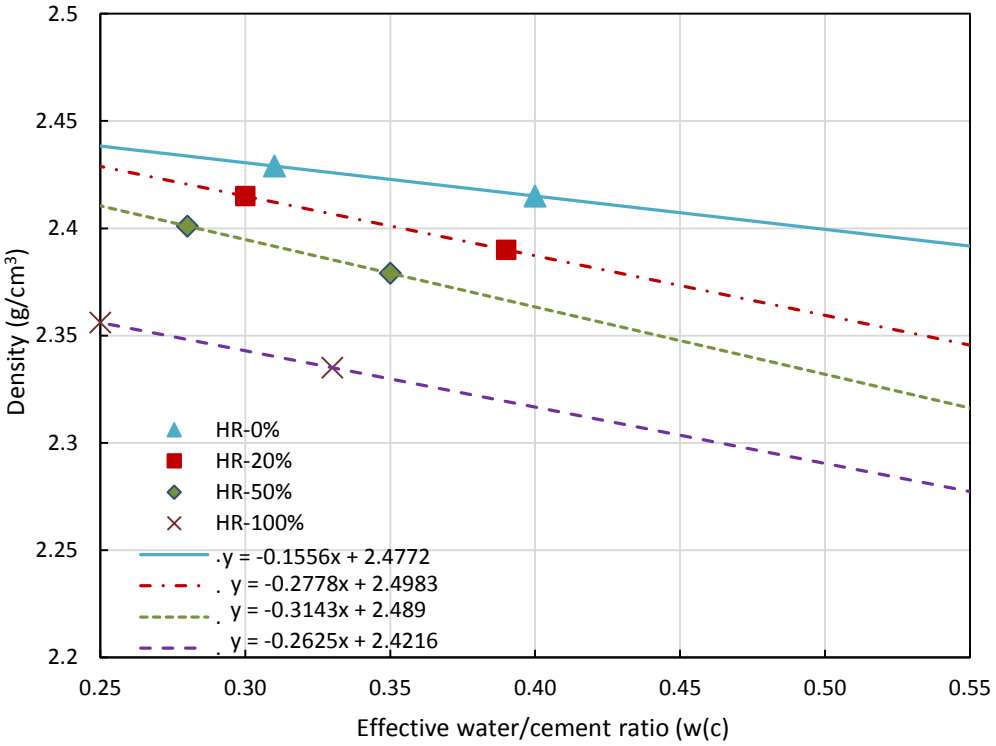

Fig. 12. Density of SCC as a function of the w/c ratio

3.11. Results of computed axial tomography

As described in the methodology, analysis using this technic have been performed comparing the properties of control concrete and concrete with 100% AR substitution. The figure shows the comparative perspective of the standard concrete and the concrete with 100% AR substitution taken from the TAC imaging treatment software.

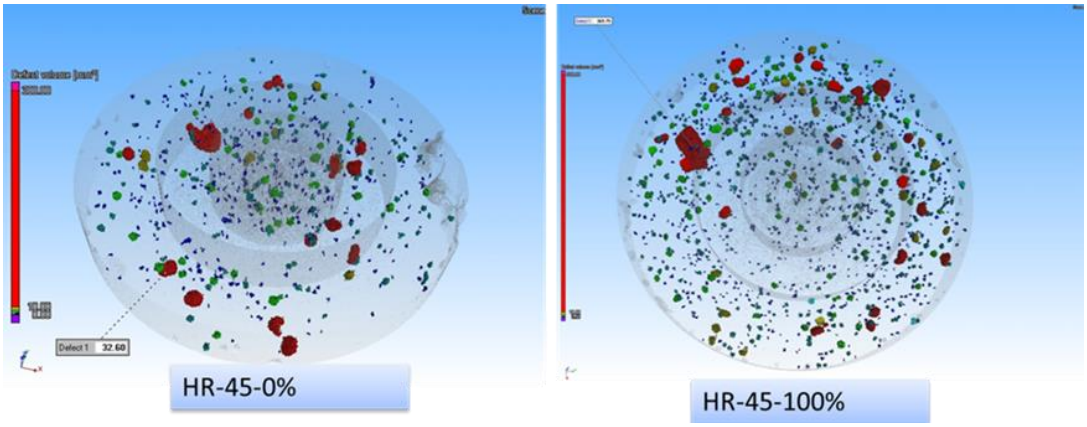

Fig. 13 3d comparison between concrete HR-45-0% and HR-45-100%.

Fig. *14* evaluates the incidence of macropores in the exterior, central and inner sectors. The area with the most macroporosity is the exterior with 100% replacement, decreasing until it equals the interior. In the interior sector it is clearly observed that the pore volume and size of the control and 100% replacement concretes are practically equal. It can also be seen that the volume of pores larger than 4 mm is greater in the concrete with AR, being lower in the control concrete.

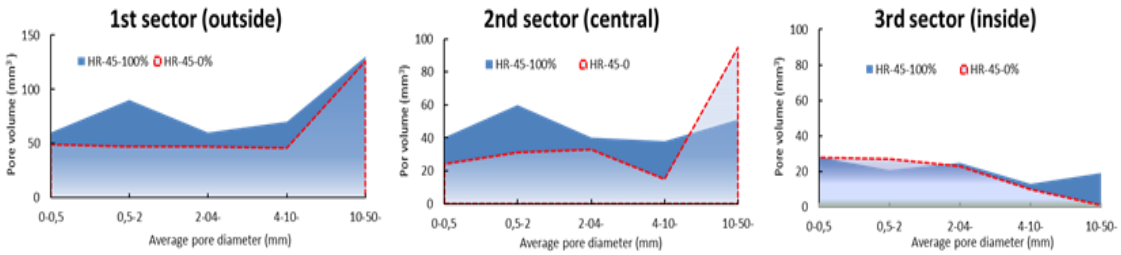

Fig. 14 Pore size and volume results in the outside, central and inside sectors.

Table 6 Quantitative value of macroporosity HR-45-0 and HR-45-100% obtained by the relationship between pore volume and apparent volume, both software. shows the quantitative pore volume values provided by the Vga studio and mimics software. The values correspond to the total percentage of pores with a size greater than 500 μm respect to the total porosity. The results of the Vga Studio software correspond to the quantitative values of pore volume, while the percentages of the Mimics software correspond to the resulting macroporosity values between the pore volume obtained by filtering in an isolated layer and the apparent volume obtained.

Table 6 Quantitative value of macroporosity HR-45-0 and HR-45-100% obtained by the relationship between pore volume and apparent volume, both software.

Type	Macroporosity (%)	
	Vga Studio	Mimics
HR-45-0% (Control)	0.45	0.78
HR-45-100%	1.80	2.01

Through the mimic software the quantification of pore volume in the standard concrete and concrete with 100% replacement is shown. The figure (Fig. 15) in 3D shows the result of the test piece, isolating the volume of the pores and the solid part.

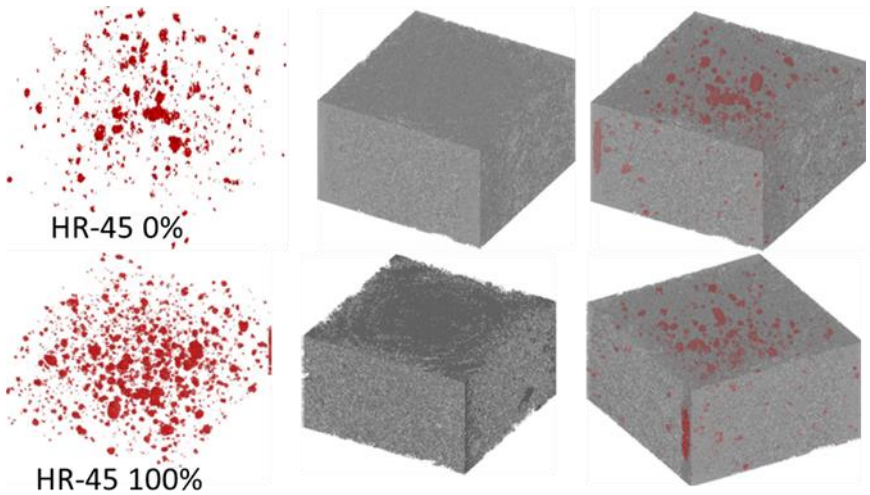

Fig. 15 The sum of pore volume and mortar is shown for HR-0% and HR-45-100%.

The micro and macro-porosity of recycled aggregate concrete was analyzed using various methods, computerized tomography (XCT), Scan electron microscopy (SEM) and Image macroporosity analysis (IMA). The results in this study showed that the total porosity obtained increases with the substitution ratio, due to the adhered mortar of the aggregate.

3.12 Mercury intrusion porosimetry results

The results of the microporosity values and the morphological characteristics of the pores are shown in Table 7.

Table 7 The results of the microporosity values and the morphological characteristics of the pores.

Type	Ømin.(nm)	Ømax.(nm)	Øprom.(nm)	Øcritical.(nm)	Volume Micropores MIP (%)
HR-45-0%	7.3	215152	91.1	79.8	8.19
HR-45-100%	7.3	215167	97.2	96.9	8.53

The graphs in Fig. *16* Cumulative intrusive volume curves.Fig. 17 Curves derived from differential intrusive volume. and Fig. 17 Curves derived from differential intrusive volume. show the accumulated volume of the micropores of the HR-45 0% and HR-45 100% concretes tested and the maximum peak of the distribution curve, which indicates the critical diameter, that is, it shows the pore size that is repeated most continuously, and that corresponds to the slope of the intrusive volume curve.

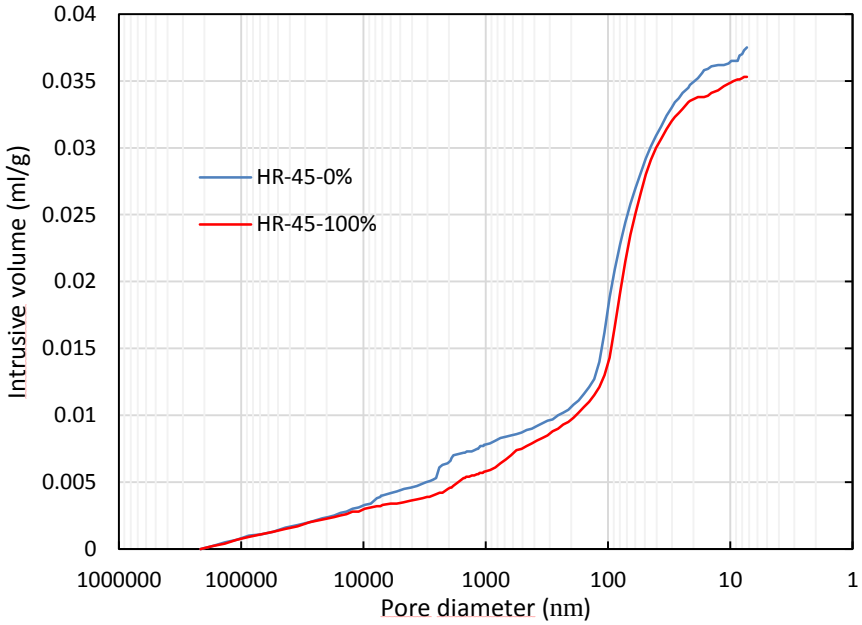

Fig. 16 Cumulative intrusive volume curves.

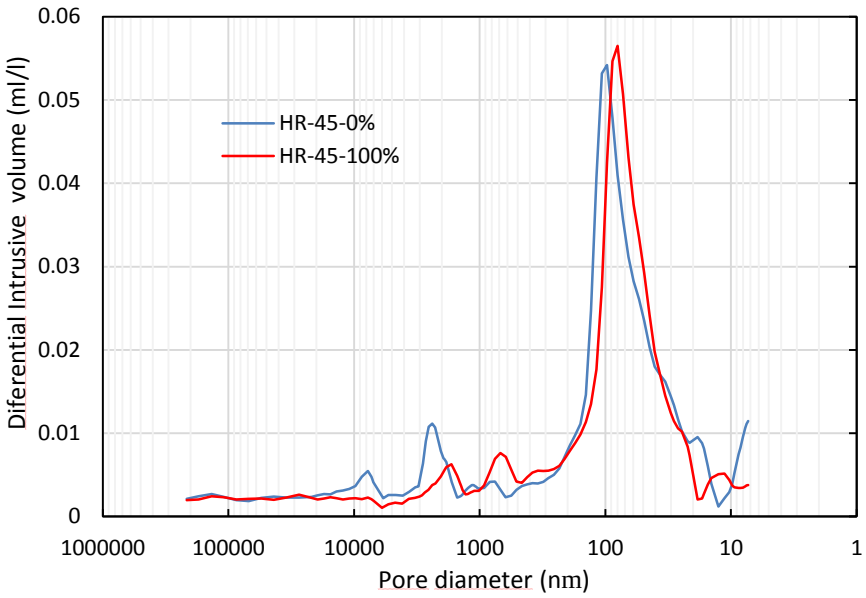

Fig. 17 Curves derived from differential intrusive volume.

The graph in Fig. 18 compares the distribution by total intrusive pore volume, where the ranges of porosity are:

- D> 1000 nm: air from the pores.
- 1000 <d <100 nm: Large capillaries, with greater effect in transport processes, and less effect of clinker hydration.
- 100 <d 10 nm: Medium capillaries that affect permeability.
- 1d <10nm: Small capillaries that affect workability

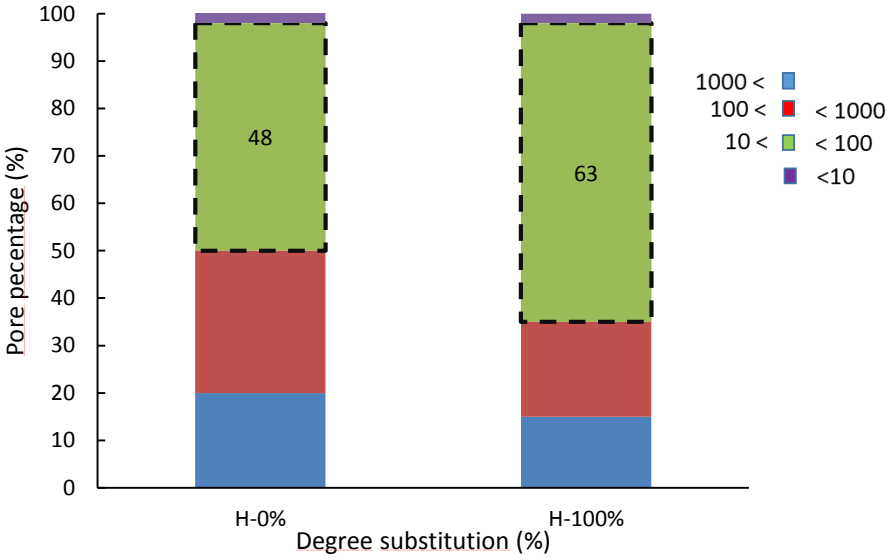

Fig. 18 Total intrusive pore volume distribution.

Based on the results, it can be concluded that the porosity results are in accordance with other studies of self-compacting concretes.

The microporosity values for the control concrete and the concrete with 100% AR substitution are very similar, given the good quality of both concretes with similar resistances, however, the highest pore content is in the range 10-100 nm (gel pores) for concrete with recycled aggregate. This is because these pores form in the cement paste and therefore a greater content of paste is incorporated through the recycled aggregates.

5. Conclusions

In view of the results obtained in this study, the conclusions that were obtained were the following:

- From the analysis of the physical and chemical properties of the recycled aggregate (RA) it can be stated that this RA is suitable for the manufacture of recycled concrete. The values are within the limits established in the Spanish Specification EHE-08. The incorporation of RA causes a decrease in the fluidity of the SCC, a small loss in strength and in modulus of elasticity of the SCC as the percentage of substitution increases.
- The incorporation of RA implies an increase in porosity, water absorption and water penetration of SCC. However, the values are within the limits for the concrete to be considered of good quality. In addition, it is observed that the curves of the concrete with a ratio of substitution of 20%, are practically similar to those of the control SCC.
- The influence of RA on the absorption of SCC is not the same for all effective w/c ratios. As w/c ratio increases, the influence of RA on the absorption coefficient is greater and when the w/c ratio is low, the differences decrease. This effect may be due to the fact that less absorbent pastes, those of lesser w/c ratio, isolate the porosity and dampen the effect that RA has on absorption.
- The density of hardened SCC and ultrasonic pulse velocity are reduced as the percentage of RA present in the mixture increases.
- The results obtained in terms of durability show a favorable response of the SCC studied, so that application would be adequate even in the most unfavorable environments.
- With the results obtained in this study, it can be seen that macroporosity and microporosity are indicators of the durability of recycled concrete since they can be correlated with capillarity and permeability, since these values are increased by including recycled aggregate. In addition, the high volume of micro pores can be associated with the transport mechanisms of gaseous pathological agents such as CO_2 and, therefore, with the loss of durability

From the results obtained in this study, it can be established that the manufacture of self-compacting concrete with recycled aggregates from precast elements is perfectly viable for different degrees of substitution, being satisfactory even with a ratio of 100%. However, the manufacturing technology of these concretes requires the use of last generation additives, such as superplasticizers.

Conflicts of Interest: Declare conflicts of interest or state "The authors declare no conflict of interest."

Acknowledgements

The authors wish to express their gratitude for having contributed to the financing of this research to: Junta de Castilla y León (Regional Government) for funding UIC-231 through project BU119P17; MINECO for funding through project BIA2014-55576- C2-1-R; and FEDER (European Regional Development Funds). Moreover, we are grateful to the precast concrete company Artepref for having collaborated with the present research work.

References

[1] EC-European-Comission, DIRECTIVE 2008/98/EC OF THE EUROPEAN PARLIAMENT AND OF THE COUNCIL of 19 November 2008 on waste and repealing certain Directives (Text with EEA relevance), n.d.

[2] BPCA, Precast Sustainability Strategy and Charter. British Precast Concrete Association., (2013).

[3] EU, REGULATION (EU) No 305/2011 OF THE EUROPEAN PARLIAMENT AND OF THE COUNCIL of 9 March 2011, Off. J. Eur. Communities. L 269 (2016) 1–15. https://doi.org/2004R0726 - v.7 of 05.06.2013.

[4] J. Sainz-Aja, I. Carrascal, J.A. Polanco, C. Thomas, Fatigue failure micromechanisms in recycled aggregate mortar by μCT analysis, J. Build. Eng. 28 (2020) 101027. https://doi.org/10.1016/J.JOBE.2019.101027.

[5] C. Thomas, J. Setién, J.A.A. Polanco, P. Alaejos, M. Sánchez De Juan, Durability of recycled aggregate concrete, Constr. Build. Mater. 40 (2013) 1054–1065. https://doi.org/10.1016/j.conbuildmat.2012.11.106.

[6] M. Bravo, J. de Brito, J. Pontes, L. Evangelista, Mechanical performance of concrete made with aggregates from construction and demolition waste recycling plants, J. Clean. Prod. 99 (2015) 59–74. https://doi.org/10.1016/J.JCLEPRO.2015.03.012.

[7] C. Thomas, J. Setién, J.A. Polanco, A.I. Cimentada, C. Medina, Influence of curing conditions on recycled aggregate concrete, Constr. Build. Mater. 172 (2018) 618–625. https://doi.org/10.1016/J.CONBUILDMAT.2018.04.009.

[8] L. Evangelista, J. Brito, Concrete with fine recycled aggregates: A review, Eur. J. Environ. Civ. Eng. 18 (2014). https://doi.org/10.1080/19648189.2013.851038.

[9] C. Thomas, J. de Brito, A. Cimentada, J.A. Sainz-Aja, Macro- and micro- properties of multi-recycled aggregate concrete, J. Clean. Prod. 245 (2020) 118843. https://doi.org/https://doi.org/10.1016/j.jclepro.2019.118843.

[10] J. Sainz-Aja, C. Thomas, J.A. Polanco, I. Carrascal, High-frequency fatigue testing of recycled aggregate concrete, Appl. Sci. 10 (2020). https://doi.org/10.3390/app10010010.

[11] J. Sainz-Aja, I. Carrascal, J.A. Polanco, C. Thomas, I. Sosa, J. Casado, S. Diego, Self-compacting recycled aggregate concrete using out-of-service railway superstructure wastes, J. Clean. Prod. 230 (2019) 945–955. https://doi.org/10.1016/J.JCLEPRO.2019.04.386.

[12] C. Thomas, J. Setién, J.A. Polanco, J. de Brito, F. Fiol, Micro- and macro-porosity of dry- and saturated-state recycled aggregate concrete, J. Clean. Prod. 211 (2019) 932–940. https://doi.org/10.1016/J.JCLEPRO.2018.11.243.

[13] F. Fiol, C. Thomas, C. Muñoz, V. Ortega-López, J.M. Manso, The influence of recycled aggregates from precast elements on the mechanical properties of structural self-compacting concrete, Constr. Build. Mater. 182 (2018) 309–323. https://doi.org/10.1016/J.CONBUILDMAT.2018.06.132.

[14] C. Thomas, J. de Brito, V. Gil, J.A. Sainz-Aja, A. Cimentada, Multiple recycled aggregate properties analysed by X-ray microtomography, Constr. Build. Mater. 166 (2018) 171–180. https://doi.org/https://doi.org/10.1016/j.conbuildmat.2018.01.130.

[15] C. Pellegrino, P. Cavagnis, F. Faleschini, K. Brunelli, Properties of concretes with Black/Oxidizing Electric Arc Furnace slag aggregate, Cem. Concr. Compos. 37 (2013) 232–240. https://doi.org/https://doi.org/10.1016/j.cemconcomp.2012.09.001.

[16] F. Lopez-Gayarre, Influencia en la variación de los parámetros de dosificación y fabricación de hormigón reciclado estructural sobre las propiedades fisico mecánicas., Universidad Oviedo., 2008.

[17] J.C. Arroyo Portero, F. Morán Cabré, Á. García Meseguer, Jimenez Montoya. Hormigón Armado.,

Madrid, 2018.

[18] M. Sánchez de Juan, Estudio sobre la utilización de árido reciclado para la fabricación de hormigón estructural., E.T.S.I. Caminos, Canales y Puertos (UPM), 2004.

[19] M. Bravo, J. de Brito, J. Pontes, L. Evangelista, Durability performance of concrete with recycled aggregates from construction and demolition waste plants, Constr. Build. Mater. 77 (2015) 357–369. https://doi.org/10.1016/J.CONBUILDMAT.2014.12.103.

[20] F.. Olorunsogo, N. Padayachee, Performance of recycled aggregate concrete monitored by durability indexes, Cem. Concr. Res. 32 (2002) 179–185. https://doi.org/10.1016/S0008-8846(01)00653-6.

[21] S. Kou, C. Poon, F. Agrela, Comparisons of natural and recycled aggregate concretes prepared with the addition of different mineral admixtures, Cem. Concr. Compos. 33 (2011) 788–795. https://doi.org/10.1016/J.CEMCONCOMP.2011.05.009.

[22] M. Martín-Morales, G.M. Cuenca-Moyano, I. Valverde-Espinosa, I. Valverde-Palacios, Effect of recycled aggregate on physical-mechanical properties and durability of vibro-compacted dry-mixed concrete hollow blocks, Constr. Build. Mater. 145 (2017) 303–310. https://doi.org/https://doi.org/10.1016/j.conbuildmat.2017.04.013.

[23] S.C. Kou, C.S. Poon, Properties of self-compacting concrete prepared with coarse and fine recycled concrete aggregates, Cem. Concr. Compos. 31 (2009) 622–627. https://doi.org/10.1016/J.CEMCONCOMP.2009.06.005.

[24] K.C. Panda, P.K. Bal, Properties of Self Compacting Concrete Using Recycled Coarse Aggregate, Procedia Eng. 51 (2013) 159–164. https://doi.org/10.1016/J.PROENG.2013.01.023.

[25] Z.J. Grdic, G.A. Toplicic-Curcic, I.M. Despotovic, N.S. Ristic, Properties of self-compacting concrete prepared with coarse recycled concrete aggregate, Constr. Build. Mater. 24 (2010) 1129–1133. https://doi.org/10.1016/J.CONBUILDMAT.2009.12.029.

[26] T. Barroqueiro, P. da Silva, J. Brito, Fresh-State and Mechanical Properties of High-Performance Self-Compacting Concrete with Recycled Aggregates from the Precast Industry, Materials (Basel). 12 (2019). https://doi.org/10.3390/ma12213565.

[27] D. Soares, J. de Brito, J. Ferreira, J. Pacheco, Use of coarse recycled aggregates from precast concrete rejects: Mechanical and durability performance, Constr. Build. Mater. 71 (2014) 263–272. https://doi.org/10.1016/J.CONBUILDMAT.2014.08.034.

[28] J.Á. Pérez Benedicto, Estudio experimental sobre propiedades mecánicas del hormigón reciclado con áridos procedentes de la no calidad, E.U. de Arquitectura Técnica (UPM), 2011.

[29] M. Velay-Lizancos, P. Vazquez-Burgo, D. Restrepo, I. Martinez-Lage, Effect of fine and coarse recycled concrete aggregate on the mechanical behavior of precast reinforced beams: Comparison of FE simulations, theoretical, and experimental results on real scale beams, Constr. Build. Mater. 191 (2018) 1109–1119. https://doi.org/https://doi.org/10.1016/j.conbuildmat.2018.10.075.

[30] AENOR, UNE-EN 1097-6. Ensayos para determinar las propiedades mecánicas y físicas de los áridos. Parte 6: Determinación de la densidad de partículas y la absorción de agua, n.d.

[31] EHE-08, Instrucción del Hormigón Estructural, (2008).

[32] AENOR, UNE-EN 933-1. Ensayos para determinar las propiedades geométricas de los áridos. Parte 1: Determinación de la granulometría de las partículas., n.d.

[33] AENOR, Tests for Geometrical Properties of Aggregates—Part 3: Determination of Particle Shape—Flakiness Index; UNE-EN 933-3:2012, 2012.

[34] AENOR, Tests for geometrical properties of aggregates - Part 4: Determination of particle shape - Shape index; UNE-EN 933-4:2008, 2008.

[35] AENOR, Tests for mechanical and physical properties of aggregates - Part 5: Determination of the water content by drying in a ventilated oven; UNE-EN 1097-5:2009, 2009.

[36] AENOR, Tests for chemical properties of aggregates - Part 1: Chemical analysis; UNE-EN 1744-1:2010, 2010.

[37] AENOR, Tests for thermal and weathering properties of aggregates - Part 2: Magnesium sulfate test; UNE-EN 1367-2:2010, 2010.

[38] AENOR, Aggregates for concrete. Determination of aggregates crushing value; UNE 83112, n.d.

[39] C. Thomas, Hormigón reciclado de aplicación estructural : Durabilidad en ambiente marino y comportamiento a fatiga, Universidad de Cantabria, 2010.

[40] A. International, ASTM C192 / C192M - 18 Standard Practice for Making and Curing Concrete Test Specimens in the Laboratory, 2018.

[41] AENOR, Testing fresh concrete - Part 1: Sampling; UNE-EN 12350-1:2009, 2009.

[42] AENOR, UNE-EN 12390-2: Ensayos de hormigón endurecido. Parte 2: Fabricación y curado de probetas para ensayos de resistencia, n.d.

[43] AENOR, Testing fresh concrete - Part 8: Self-compacting concrete - Slump-flow test; UNE-EN 12350-8:2011, 2011.

[44] AENOR, UNE-EN 12390-3. Ensayos de hormigón endurecido. Parte 3: Determinación de la resistencia a compresión de probetas, España, 2003.

[45] AENOR, Testing hardened concrete - Part 6: Tensile splitting strength of test specimens; UNE-EN 12390-6:2010, 2010.

[46] AENOR, Testing hardened concrete - Part 5: Flexural strength of test specimens; UNE-EN 12390-5:2009, 2009.

[47] AENOR, Concrete tests. Determination of the Modulus of Elasticity in compression; UNE 83316., 1996.

[48] AENOR, Testing fresh concrete - Part 2: Slump-test; UNE-EN 12350-2:2009, 2009.

[49] A. International, ASTM C642 - 13; Standard Test Method for Density, Absorption, and Voids in Hardened Concrete, 2013.

[50] AENOR, Testing hardened concrete - Part 8: Depth of penetration of water under pressure; UNE-EN 12390-8:2009, 2009.

[51] AENOR, UNE-EN 12390-7. Ensayos de hormigón endurecido. Parte 7: Densidad del hormigón endurecido., España, n.d.

[52] AENOR, Testing concrete - Part 4: Determination of ultrasonic pulse velocity; UNE-EN 12504-4., 2006.

[53] A.M. Neville, J.J. Brooks, Concrete Technology, Longman Scientific & Technical, 1987.

[54] D. Abrams, Design of Concrete Mixtures, Structural Materials Research Laboratory, Lewis Institute, Chicago., 1919.

[55] S.W. Tabsh, A.S. Abdelfatah, Influence of recycled concrete aggregates on strength properties of concrete, Constr. Build. Mater. 23 (2009) 1163–1167. https://doi.org/10.1016/j.conbuildmat.2008.06.007.

[56] T.-Y. Tu, Y.-Y. Chen, C.-L. Hwang, Properties of HPC with recycled aggregates, Cem. Concr. Res. 36 (2006) 943–950. https://doi.org/10.1016/J.CEMCONRES.2005.11.022.

[57] B. González Fonteboa, Hormigones con áridos reciclados procedentes de demoliciones: Dosificaciones, propiedades mecánicas y comportamiento estructural a cortante, UNIVERSIDADE DA CORUÑA, 2002.

[58] T. Ikeda, S. Yamame, A. Sakamoto, Strengths of concrete containing Recycled concret aggregate Demolition and Reuse of Concrete Masonry Japan, (1988) 585–594.

[59] M. Sánchez, P. Alaejos, Estudio sobre las propiedades del hormigón fabricado con áridos reciclados, Monografía, CEDEX, Madrid, 2012.

[60] M. Etxeberria, E. Vázquez, A. Marí, M. Barra, Influence of amount of recycled coarse aggregates and production process on properties of recycled aggregate concrete, Cem. Concr. Res. 37 (2007) 735–742. https://doi.org/10.1016/J.CEMCONRES.2007.02.002.

[61] Comite Euro-International du Bèton, Strategies for Testing and Assessment of Concrete Structures affected by Reinforcement Corrosion., (1988) 184.

[62] V. Andrea, Durabilidad en hormigones armados con árido reciclado. Una evaluación de la corrosión en ambiente marino, Universitat Politècnica de València, Valencia, 2012.

[63] E.A. Whitehurst, Soniscope tests concrete structures, [Portland Cement Association], Chicago, 1951.

[64] C. Thomas, J. Setién, J.A. Polanco, Structural recycled aggregate concrete made with precast wastes, Constr. Build. Mater. 114 (2016) 536–546. https://doi.org/10.1016/J.CONBUILDMAT.2016.03.203.

[52] AENOR, Testing concrete - Part 4: Determination of ultrasonic pulse velocity; UNE-EN 12504-4., 2006.

[53] A.M. Neville, J.J. Brooks, Concrete Technology, Longman Scientific & Technical, 1987.

[54] D. Abrams, Design of Concrete Mixtures, Structural Materials Research Laboratory, Lewis Institute, Chicago., 1919.

[55] S.W. Tabsh, A.S. Abdelfatah, Influence of recycled concrete aggregates on strength properties of concrete, Constr. Build. Mater. 23 (2009) 1163–1167. https://doi.org/10.1016/j.conbuildmat.2008.06.007.

[56] T.-Y. Tu, Y.-Y. Chen, C.-L. Hwang, Properties of HPC with recycled aggregates, Cem. Concr. Res. 36 (2006) 943–950. https://doi.org/10.1016/J.CEMCONRES.2005.11.022.

[57] B. González Fonteboa, Hormigones con áridos reciclados procedentes de demoliciones: Dosificaciones, propiedades mecánicas y comportamiento estructural a cortante, UNIVERSIDADE DA CORUÑA, 2002.

[58] T. Ikeda, S. Yamame, A. Sakamoto, Strengths of concrete containing Recycled concret aggregate Demolition and Reuse of Concrete Masonry Japan, (1988) 585–594.

[59] M. Sánchez, P. Alaejos, Estudio sobre las propiedades del hormigón fabricado con áridos reciclados, Monografía, CEDEX, Madrid, 2012.

[60] M. Etxeberria, E. Vázquez, A. Marí, M. Barra, Influence of amount of recycled coarse aggregates and production process on properties of recycled aggregate concrete, Cem. Concr. Res. 37 (2007) 735–742. https://doi.org/10.1016/J.CEMCONRES.2007.02.002.

[61] Comite Euro-International du Bèton, Strategies for Testing and Assessment of Concrete Structures affected by Reinforcement Corrosion., (1988) 184.

[62] V. Andrea, Durabilidad en hormigones armados con árido reciclado. Una evaluación de la corrosión en ambiente marino, Universitat Politècnica de València, Valencia, 2012.

[63] E.A. Whitehurst, Soniscope tests concrete structures, [Portland Cement Association], Chicago, 1951.

[64] C. Thomas, J. Setién, J.A. Polanco, Structural recycled aggregate concrete made with precast wastes, Constr. Build. Mater. 114 (2016) 536–546. https://doi.org/10.1016/J.CONBUILDMAT.2016.03.203.